Available online at www.sciencedirect.com
SCIENCE DIRECT
Journal of Power Sources 152 (2005) 168–174
JOURNAL OF POWER SOURCES
www.elsevier.com/locate/jpowsour

Thermal cycle stability of a novel glass–mica composite seal for solid oxide fuel cells: Effect of glass volume fraction and stresses

Yeong-Shyung Chou *, Jeffry W. Stevenson, Prabhakar Singh

Pacific Northwest National Laboratory, Materials Division, K2-44, P.O. Box 999, Richland, WA 99354, USA

Received 22 February 2005; received in revised form 10 March 2005; accepted 11 March 2005
Available online 9 June 2005

Abstract

A novel glass–mica composite seal was developed based on a previously reported concept of "infiltrated" mica seals for solid oxide fuel cells. Ba–Al–Ca silicate sealing glass powder and Phlogopite mica flakes were mixed at glass volume fractions of 10–50 vol.% to make the glass–mica composite seals. The seals were leak tested for short-term thermal cycle stability as a function of glass volume fraction. Composite seals with 10 and 20 vol.% glass were also leak tested under compressive stresses from 3 to 100 psi and helium pressures of 0.2 or 2 psi. Post-mortem microstructure analyses were used to characterize the fracture (leak path) of the glass–mica composite seals and were related to the high temperature leakages. Open circuit voltage tests on dense 8YSZ electrolyte with the glass–mica composite seal showed very good thermal cycle stability over 250 cycles with minute (<1%) voltage drop.

Keywords: Compressive seal; Mica; Leak test; Thermal cycle; SOFC

1. Introduction

Among many technical hurdles hindering the advancement of solid oxide fuel cells (SOFC), a durable stack sealant or sealants is at or near the top on the list. The sealant needs to be not only thermally and chemically stable in the dual oxidizing and reducing environment, but also to be electrical insulating and mechanically strong for long-term operation of over 40,000 h. The problem becomes more challenging when thermal cycle stability is also required for planar stacks in which dissimilar SOFC components are sealed together. The sealants have to survive hundreds to several thousands of thermal cycles during life service. To date, several different approaches for SOFC seals have been investigated, including rigid glass, glass–ceramic, and fiber-reinforced glass seals [1–6], compressive mica seals [7–10], and metallic seals such as active brazing alloys or silver wire [11–14]. In our previous studies, we have identified the major leak paths of conventional compressive mica seals to be at the interfaces between the mica and mating materials. Based on this finding, the "hybrid" mica seal was proposed by adding glass or metal interlayers at these interfaces. As a result, the leak rates were reduced hundreds to thousands of times as compared to the conventional mica seals [1,2]. However, the leak rates tended to increase rapidly to $\sim(2–5) \times 10^{-2}$ sccm cm^{-1} (standard cubic centimeters per minute per centimeter of seal length) during the initial thermal cycles. To further reduce the leakage, we developed "infiltrated" mica seals using boric acid or bismuth nitrate [10]. The concept is shown in Fig. 1 with boric acid or bismuth nitrate infiltrated at the voids between mica flakes such that at elevated temperatures they formed a wetting liquid and blocked the leak path. The leak rates were greatly reduced to $\sim10^{-3}$ sccm cm^{-1} as compared to hybrid micas ($\sim(2–5) \times 10^{-2}$ sccm cm^{-1}); however, both the boric acid and the bismuth nitrate were not considered to offer long-term stability in the SOFC environments [10]. In this paper, we present a modified approach in which glass

* Corresponding author. Tel.: +1 509 375 2527; fax: +1 509 372 2186.
E-mail address: yeong-shyung.chou@pnl.gov (Y.-S. Chou).

0378-7753/$ – see front matter © 2005 Elsevier B.V. All rights reserved.
doi:10.1016/j.jpowsour.2005.03.213

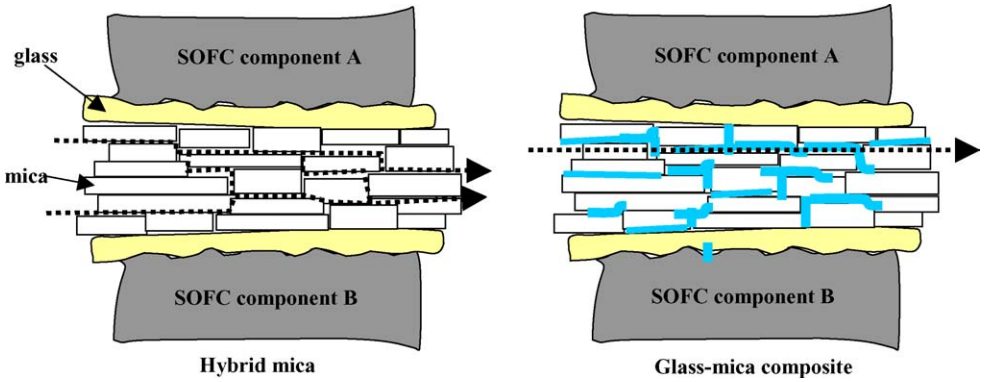

Fig. 1. Schematic showing the glass–mica composite seals with glass filler between large mica flakes (right), and the original hybrid mica seal based on mica paper without glass filler (left), between two SOFC components. The leak paths in hybrid mica are considered 3D through voids between mica flakes (dotted lines), and 2D for glass–mica composite seals.

powders were mixed with large Phlogopite mica flakes to form a glass–mica composite seal. Leakage was measured versus short-term thermal cycles for glass–mica composite seals with 20–50 vol.% glass. Glass–mica composite seals with 10 and 20 vol.% glass were also evaluated to determine the effect of applied compressive stress on the short-term thermal cycle leakage. Post mortem microstructure analyses were used to characterize the degradation and failure of the hybrid glass–mica composite seals. In addition, the composite seals were tested on a dense 8YSZ (8% yttria stabilized zirconia) electrolyte for open circuit voltage (OCV) during long-term thermal cycling.

2. Experimental

2.1. Materials and processing

A Ba–Al–Ca silicate glass was used as one of the two components of the glass–mica composite seals. The glass was developed at Pacific Northwest National Laboratory as a sealing glass for SOFCs with coefficient of thermal expansion (CTE) closely matched with Ni/YSZ anode-supported 8YSZ electrolyte membranes (CTE ~ 12.5 ppm $^{\circ}C^{-1}$) [15]. The glass was made from constituent oxides, melted and attrition milled for 2 h in ethanol. After oven drying (~110 °C), the glass powders were mixed with an organic binder (Duramax B-1050, Rohm Haas, PA) in deionized water to form a solution containing ~3–5% binder. Phlogopite mica flakes in a paper form (Cogemica PP159, Cogebi, Inc., NH) were cut into ~4.5 in. × 4.5 in. (11.4 cm × 11.4 cm) squares and placed on top of a Mylar film within an aluminum frame. The glass-binder aqueous solution was then poured into the aluminum frame and shaken to disperse the large mica flakes. The mixed slurry was dried at ambient conditions overnight. The glass volume fractions in the glass–mica composite were 10, 20, 30, and 50 vol.%. A separate glass tape was also made by tape casting the Ba–Al–Ca silicate glass powders in an organic solvent system. After drying, the glass tape had a thickness about 150–200 μm. The dried glass tapes were cut into the desired geometry and used as interlayers for hybrid mica leak testing.

2.2. Leak testing and open circuit voltage

The as-made glass–mica composite sheets were cut into 2 in. × 2 in. (5 cm × 5 cm) frames and sandwiched between two glass tapes to form the "hybrid" mica seal for leak testing [7,8]. The assembly was then pressed between an Inconel600 fixture (2 in. × 2 in.) and a dense alumina substrate (ADS-96R, CoorsTek, CO) at a constant stresses of 6 psi (41 kPa) using a dead weight. The choice of Inconel600 was based on its superior oxidation resistance and mechanical strength at elevated temperatures. The large CTE mismatch between the two materials (Inconel600: CTE = ~16.7 ppm $^{\circ}C^{-1}$ RT to 800 °C average, alumina: CTE = ~8.5–9 ppm $^{\circ}C^{-1}$) was an important part of the test. Rigid seals such as glass or brazes would not be expected to survive thermal cycling under these conditions, whereas compressive mica seals have the potential for sealing SOFC components with large CTE mismatch since the flakes are not rigidly bonded with each other. Furthermore, the large mica flakes (~1–2 mm in size and ~10–20 μm thick) could also easily cleave along their basal planes. The high temperature leak rate was measured with ultra-high purity helium and was determined by monitoring the pressure change with time. The details of the leak rate calculation and experimental setup are given in Refs. [7,8]. In the current 800 °C leak tests, two helium pressures were used: 0.2 psi (~1.4 kPa) and 2 psi (~14 kPa). A pressure of 0.2 psi is likely to be close to actual planar SOFC operations, while 2 psi may be considered an upper limit. In addition, we also selected two glass–mica composites to study the effect of compressive stresses on the leakage: 10 and 20 vol.% glass. The stresses studied were in two regions: low stress region (3, 6, and 12 psi or 20, 41, and 82 kPa) and high stress region (25, 50, and 100 psi or 170, 340, and 680 kPa). The temperature profiles of the thermal cycling are given in Ref. [17]. During the whole test (except when measuring the leakage with

helium) moist (~3% H_2O), dilute hydrogen (~2.7% H_2/bal. Ar) was flowing at a constant rate to simulate the SOFC anode environment. Optical and scanning electron microscopy was also used for post mortem microstructure analyses. The glass (20 vol.%)–mica composite seals were also tested for thermal cycle stability using OCV measurements. For those measurements, a dense 8YSZ electrolyte plate (2 in. × 2 in.) was screen printed with silver paste and sealed with the hybrid composite seals at a stress of 26 psi (176 kPa). The details of the experimental setup and temperature profiles of the OCV test are given in Ref. [18].

3. Results and discussion

3.1. Effect of glass volume on the leak rate during thermal cycling

The effect of glass volume fraction on the 800 °C leakage of the hybrid glass–mica composite seals during thermal cycling is shown in Fig. 2A. For comparison, results for a hybrid mica seal without glass infiltration (i.e., glass volume fraction = 0 vol.%, see Fig. 1A) is also included. The sample was pressed at a low stress of 6 psi and leak tested at a helium differential pressure of 0.2 psi. It is interesting to note that before thermal cycling, the 800 °C leak rates were ~0.019 sccm cm^{-1} (glass = 0 vol.%), ~0.020 sccm cm^{-1} (20 vol.%), ~4×10^{-4} sccm cm^{-1} (30 vol.%), and ~2×10^{-4} (50 vol.%). At glass volume fraction ≥ 30 vol.%, the 800 °C leak rates are close to the detection limit of the leak tester, i.e., ~10^{-4} sccm cm^{-1}. The leak rate of ~10^{-4} sccm cm^{-1} is also equivalent to a typical glass seal before thermal cycling when measured with the current fixtures. This suggests that the glass filled most of the voids, formed a continuous network and effectively blocked the continuous 3D leak path (Fig. 1A) between mica flakes at volume fraction ≥ 30 vol.%. This glass volume fraction of 30% appears to be higher than one would expect to need to fill the void space of a compact of large flat flakes with preferred orientation. This is likely due to the uneven distribution of mica flakes; some of the large mica flakes (1–2 mm in dimensions) are difficult to disperse in aqueous slurry. Moreover, the glass used was a glass–ceramic, i.e., it tends to nucleate and crystallize into a rigid ceramic phase with some residual glass. The low applied compressive stress of 6 psi may not have been enough to squeeze out excess glass and still maintain a continuous network at a lower glass fraction. Upon thermal cycling, the high temperature leakage increased rapidly during the initial thermal cycles, but tended to flatten out in the subsequent thermal cycles. The rapid increase in leakage is attributed to newly formed leak paths, likely near the Inconel600 interface where the largest CTE mismatch is present (the CTE of Phlogopite mica is ~11 ppm $°C^{-1}$ (RT to 800 °C average), and ~12 ppm $°C^{-1}$ for the Ba–Ca–Al silicate glass interlayer). After 25–30 thermal cycles, the 800 °C leak rates were ~0.05–0.06 sccm cm^{-1} (glass = 0 vol.%), ~0.03–0.04 sccm cm^{-1} (20 vol.%), ~0.01 sccm cm^{-1} (30 vol.%), and ~0.009 sccm cm^{-1} (50 vol.%). It is evident that the higher glass content resulted in lower leak rates. Compared to the leak rates of hybrid mica without glass infiltration, the lower leakage of glass (30–50 vol.%)–mica composite seals suggest the blockage of leak path (voids) though mica flakes by the presence of the crystallized glass–ceramic.

3.2. Leak test at high helium pressure of 2 psi

The leak tests described above were conducted at a small pressure difference of 0.2 psi across the mica seal. This low pressure drop may be appropriate for planar SOFC stacks with Ni/YSZ anode-supported thin electrolyte cells due to the low strength and creep resistance of Ni/YSZ anode for long-term operation at ~750–800 °C and SOFC environments [16]. In addition, the use of ferritic stainless steel and similar alloys as the interconnect materials would also drive down the operating temperatures such that thinner membranes are preferred for better kinetics and less oxidation problems for metals. As a result, higher operating gas pressures may not be practical. Nevertheless, we have also measured the high temperature leak rates at a high differential pressure of 2 psi helium. Such a pressure may provide as an upper limit for the planar SOFCs when the problems mentioned earlier are not important. The leakage versus thermal cycles of the three glass–mica composites is shown in Fig. 2B. It is evident that the leak rates are larger at higher differential pressures. For example, the leak rates after 20–30 thermal cycles are ~0.28 sccm cm^{-1} (20 vol.%), ~0.05 sccm cm^{-1} (30 vol.%), and ~0.04 sccm cm^{-1} (50 vol.%) for the differential pressure of 2 psi. The composite seals with glass volume fraction ≥ 30 vol.% also showed a plateau, consistently with data tested at 0.2 psi (Fig. 2A). However, the glass–mica composite seal with 20 vol.% glass showed a continuous increase in leak rate over the 30 thermal cycles, unlike the leak behavior when tested at a low helium differential pressure of 0.2 psi (Fig. 2A). The cause will be discussed in the following microstructure analysis section.

3.3. Effect of applied compressive stress on leakage during thermal cycling

The effect of applied compressive stress was also investigated on the hybrid glass–mica composite seals during short-term thermal cycling. Composite seals with glass volume fraction of 10 and 20 vol.% were studied at two stress regions: low stresses of 3, 6, and 12 psi, and high stresses of 25, 50, and 100 psi. For these tests, a helium pressure of 0.2 psi was used for low compressive stresses, and a differential pressure of 2 psi was used for high compressive stresses. The use of 2 psi

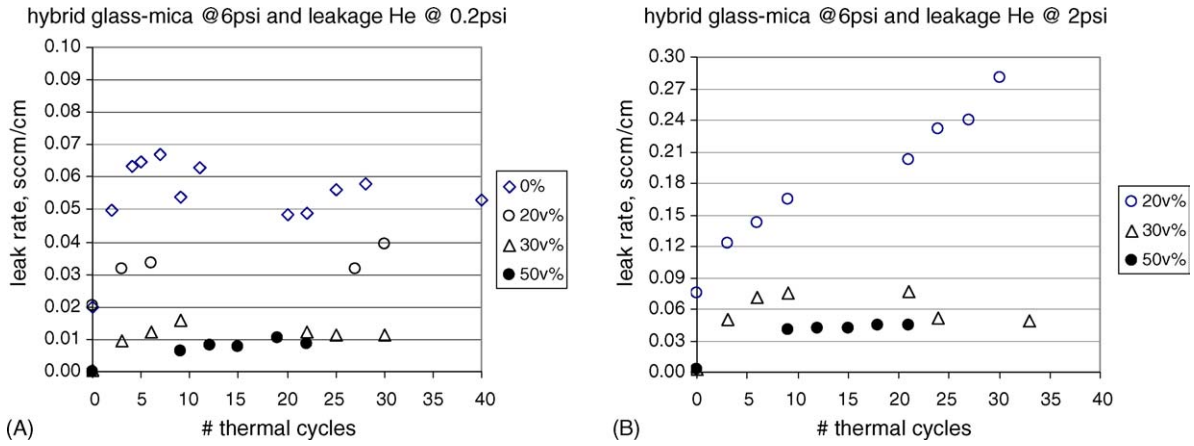

Fig. 2. Effect of glass volume fraction on the high temperature leakage of the hybrid glass–mica composite seals. The glass is a Ba–Ca–Al silicate glass which crystallizes into a rigid glass–ceramic. The hybrid seal was pressed at a stress of 6 psi and tested with helium at 0.2 psi (A) and 2 psi (B).

helium for high compressive stresses was due to very low leakage if measured by helium at 0.2 psi. For planar SOFC stacks of actual size (e.g., 8 in. × 8 in.) the total sealing areas could be around 10 in^2, so that a compressive stress of ≥100 psi would require ≥1000 lbs of load to be applied to the stack. Such a high load would require some type of loading system and is undesirable from a cost and engineering point of view, so compressive stresses of 3 and 100 psi therefore were chosen as a lower and upper limit of mica-based seals for SOFC stacks. The leak rates versus thermal cycles are shown in Fig. 3 for glass (20 vol.%)–mica composite seal at low stresses, Fig. 4 for glass (20 vol.%)–mica composite seal at high stresses, and Fig. 5 for glass (10 vol.%)–mica composite seal at high stresses. It is clear that the higher compressive stresses result in the lower leak rates. In the low stress region (3–12 psi) of the glass (20 vol.%)–mica composite, the leak rates are 0.011–0.015 sccm cm^{-1} after 36 thermal cycles for a stress of 12 psi, and ∼0.04–0.05 sccm cm^{-1} for a stress of 3 psi after 28 thermal cycles (Fig. 3). The composite seals all show good thermal cycle stability with leak rates remaining fairly constant or increasing slowly with thermal cycles. At higher compressive stresses (25–100 psi), the leak rates are much smaller for the composite seal with 20 vol.% glass (Fig. 4). For example, the leak rates are less than 10^{-3} sccm cm^{-1} after about 25 thermal cycles for 50 and 100 psi. The leak rates appear to decrease with increasing thermal cycles for these two stresses states as compared to 25 psi where the leak rates increase with thermal cycles. For the glass (10 vol.%)–mica composite at the same stress region, lower leak rates are obtained only when stress is 100 psi (Fig. 5). The leak rates tend to increase with increasing thermal cycles for both compressive stresses of 25 and 50 psi. The results of glass–mica composites under high stress region indicate that higher stresses are needed for low glass volume fraction to have low leak rates and thermal cycle stability.

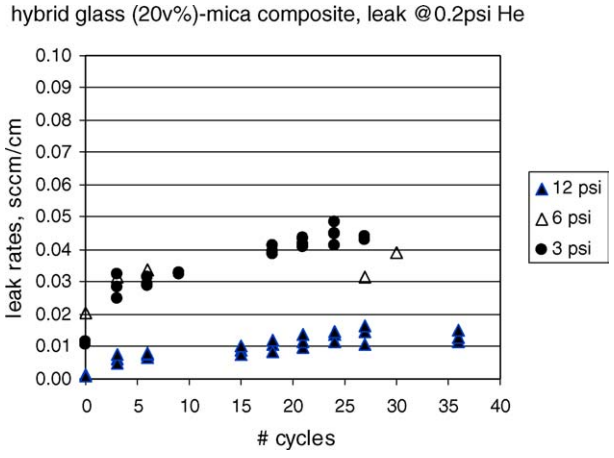

Fig. 3. Effect of compressive stresses on the high temperature leakage of the hybrid glass (20 vol.%)–mica composite seals during thermal cycling. Note the leak rate was measured with helium at a differential pressure of 0.2 psi.

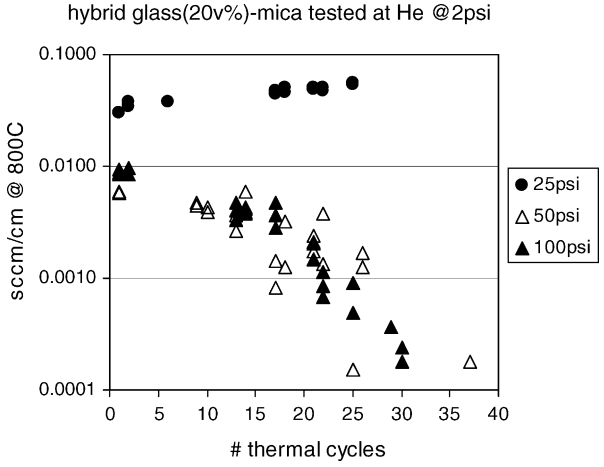

Fig. 4. Effect of compressive stresses on the high temperature leakage of the hybrid glass (20 vol.%)–mica composite seals during thermal cycling. Note the leak rate was measured with helium at a differential pressure of 2 psi.

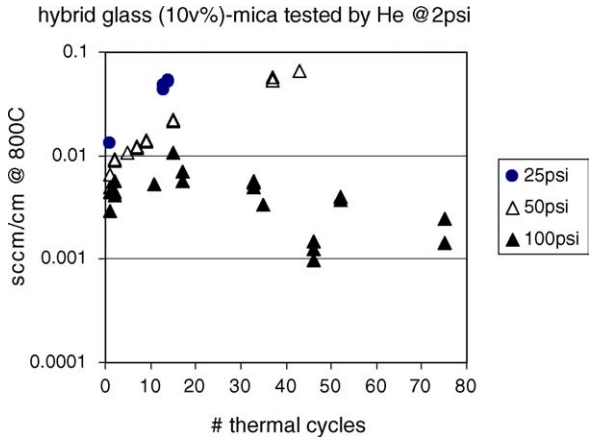

Fig. 5. Effect of compressive stresses on the high temperature leakage of the hybrid glass (10 vol.%)–mica composite seals during thermal cycling. Note the leak rate was measured with helium at a differential pressure of 2 psi.

The continuous decrease of leak rates from 10^{-2} to 10^{-3} and 10^{-4} sccm cm^{-1} suggests some reaction of the Ba–Ca–Al silicate glass with the Phlogopite mica ($KMg_3(AlSi_3O_{10})(F, OH)_2$). For planar SOFC stacks, a leak rate corresponding to $\leq$1% of the total fuel flow for a 6 in. × 6 in. cell at a differential pressure of 0.147 kPa (~0.1 psi) was proposed by the Solid Energy Convergence Alliance as a criterion for sealant development. Using the last leakage data of the glass (20 vol.%)–mica composite seals at various compressive stresses from Fig. 3 (i.e., leak rate data at thermal cycle #27, #30, and #36 for stresses of 3, 6, and 12 psi, respectively), the total fuel loss was estimated to be ~0.5% (3 psi), ~0.4% (6 psi), and ~0.1% (12 psi) for a cell of 6 in. × 6 in. (with a power density of 0.5 W cm^{-2} and operated at 0.7 V, 800 °C, and 80% fuel utilization with pure hydrogen and air). This simple calculation suggests that the glass–mica seals are suitable as the sealants for SOFC stacks, although it should be noted that the calculation requires the assumption that the same leak rates observed in our relatively small (2 in. × 2 in.) test seals would be obtained in the full size stacks. This assumption is reasonably as long as the stack is designed to deliver the required compressive stress uniformly to all stack seals.

3.4. Fracture surface and microstructure analysis

After the thermal cycling tests, all the hybrid glass–mica composite seals were easily detached from the Inconel600 test fixture. This was expected since the largest CTE mismatch was present near the Inconel600 side (rather than the alumina substrate side) and therefore fracture would be expected to occur along the interface on the Inconel600 side. Fig. 6A shows the typical fracture surface of the glass (20 vol.%)–mica composite seals pressed at 6 psi after 30 thermal cycles, and Fig. 6B for the glass (50 vol.%)–mica composites after 22 thermal cycles. Fig. 7 shows a higher magnification of a typical fracture surface of the pressed region in Fig. 6A. It was evident the majority of fracture occurred between mica flakes, which remained intact and reflective. However, several darker sections were observed in the glass (20 vol.%)–mica composite seal of Fig. 6A. In these regions, fracture occurred along the interface between the Inconel600 fixture and the glass interlayer where no reflective mica flakes were present. The fracture surfaces of other hybrid glass–mica composites with 30 and 50 vol.% of glass showed similar reflective mica surfaces without the non-reflective dark sections. On higher SEM magnification of the glass (20 vol.%)–mica composite seals, the fracture surfaces showed distinct difference in morphology. The fracture surface is much smoother for fracture occurring between mica flakes (Fig. 8A) than for fracture occurring within the glass interlayer or at the interface between the metal and the glass. In the second case, the roughness of the fracture surface corresponded to the grain sizes of the crystallized Ba–Ca–Al silicate glass–ceramic (Fig. 8B). This suggests that the dark fracture sections in Fig. 6A were likely the cause for the continuous increase in leak rates with increasing thermal cycles when tested with helium at 2 psi (Fig. 2B), especially the section which covers the whole sealing width (arrow in Fig. 6A). It is believed that two microstructurally flat fracture surfaces can closely match with each other when heating back to the elevated temperatures. Theoretically, the fracture planes in mica flakes can be atomically flat since they tend to fracture along the cleavage planes. As a result, the leak path would be small and low leak rates should result. On the other hand, the rough fracture surfaces which result when fracture occurs through the glass interlayer or at the glass/metal interface will not closely match with each other when heating back to elevated temperatures. It is known that fracture in brittle ceramics is not reversible, i.e., there are elastic energies lost during the fracturing process, and grains are pulled out, re-oriented or microfractured. Consequently, the leak paths are more open and result in higher leak rates. It is not clear why glass–mica composites with higher glass contents (30 and 50 vol.%) did not result in the fracture along the metal/glass interface or through the glass interlayers.

3.5. Open circuit voltage versus long-term thermal cycling

An open circuit voltage test was also conducted on a glass (20 vol.%)–mica composite seal to further evaluate the long-term thermal cycle stability. The glass–mica composite seal was sandwiched between the Inconel600 fixture and a dense 8YSZ electrolyte plate (2 in. × 2 in.) printed with Ag as electrodes. The assembly was thermally cycled between ~100 and 800 °C in a flowing low hydrogen fuel of ~2.7% H_2/bal. Ar + ~3% H_2O. The results of OCV at 800 °C versus the number of thermal cycles are shown in Fig. 9. It is evident that the glass–mica composites showed excellent thermal cycle stability with constant OCV of ~0.927–0.933 V at 800 °C over 250 thermal cycles. The theoretical OCV for a hermetic

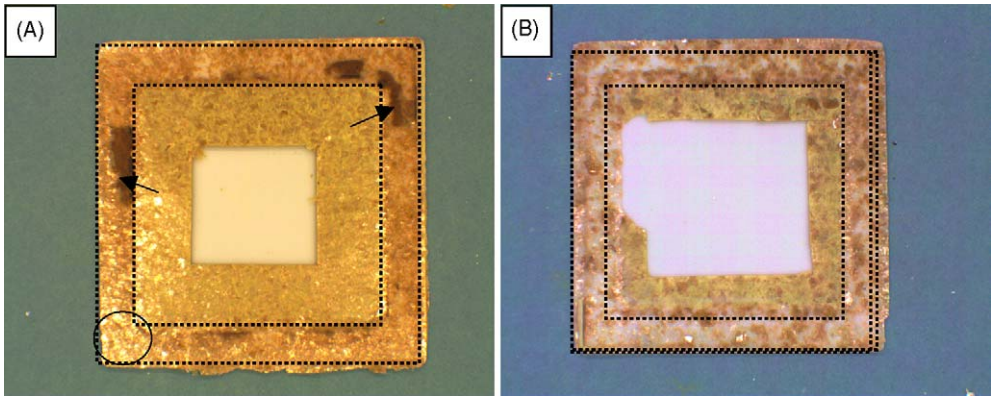

Fig. 6. Fracture surface of the thermally cycled hybrid glass–mica composite seals pressed (within dotted lines) between an Inconel600 fixture and an alumina substrate at 6 psi. The fracture occurred along the interface near the Inconel600 side where the largest CTE mismatch was present. (A) Glass (20 vol.%)–mica after 30 thermal cycles, and (B) glass (50 vol.%)–mica after 22 thermal cycles.

seal with gases of ∼2.6–2.7% H_2/bal. Ar + ∼3% H_2O versus air was calculated to be 0.0933–0.935 V at 800 °C. The measured OCVs are very close to the theoretical OCVs, indicating very low leakage through the glass–mica composite seals. In addition to the direct measurement of leak rates at elevated temperatures, one can also calculate the leakage from measured OCVs, assuming no temperature variations across the 2 in. × 2 in. sample and no voltage drop from electrical contacts. Using the lower measured OCV of 0.927 V at 800 °C and a fuel (2.71% H_2/bal. Ar + 3% H_2O) flow rate of 63 sccm, the air leakage into the fuel side was calculated to be ∼0.018 sccm cm^{-1}. The measured leak rates for a glass (20 vol.%)–mica composite seal at a compressive stress of 25 psi and a differential pressure of 2 psi was about 0.055 sccm cm^{-1} (Fig. 4). The leakage at a differential pressure of 0.2 psi was not experimentally measured but can be estimated to be 0.008–0.011 (using the ratios of leak rate at 2 psi to leak rate at 0.2 psi of the 20 vol.% composites pressed at 6 psi in Fig. 2A and B), which is fairly consistent with the calculated leak rate from the OCV test. Overall, the measured OCV clearly demonstrated the excellent sealing capability and thermal cycle stability of the glass–mica composite seals.

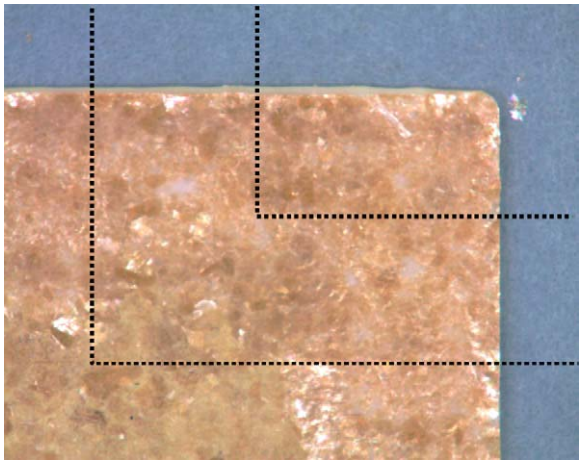

Fig. 7. Higher magnification of the fracture surface of the thermally cycled hybrid glass (20 vol.%)–mica composite seal (circle in Fig. 6A). The pressed regions are within the dotted lines. Note the reflective mica flakes are present on most of the fracture surface.

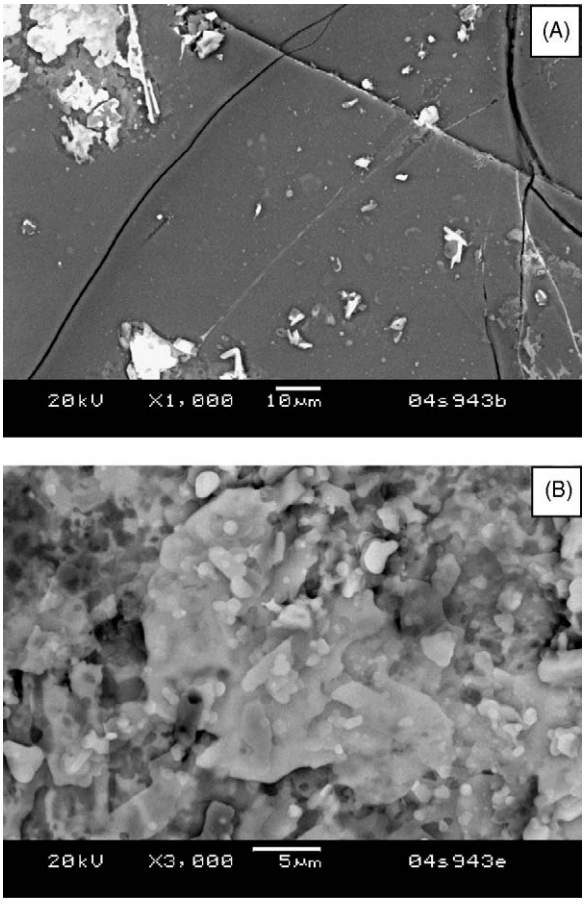

Fig. 8. SEM micrographs show the fracture surface of the hybrid glass (20 vol.%)–mica composites seals after 30 thermal cycles. The sample was pressed at a compressive stress of 6 psi. (A) Fracture surface on mica flakes, and (B) fracture surface morphology on the crystallized Ba–Ca–Al silicate glass–ceramic.

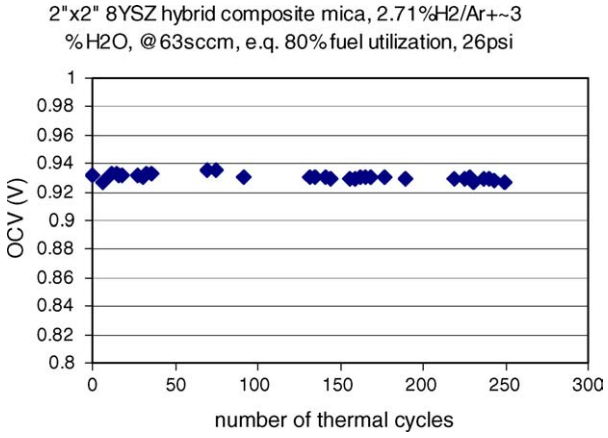

Fig. 9. Effect of thermal cycling on the open circuit voltage of a glass (20 vol.%)–mica composite in hybrid form pressed at a stress of 26 psi on a dense 8YSZ electrolyte plate (2 in. × 2 in.). The sample was exposed to ambient air and a flowing gas of ∼2.7% H_2/bal. Ar + ∼3% H_2O during cycling between ∼100 and 800 °C and OCV was measured at 800 °C. The Nernst voltage was calculated to be 0.934 V.

4. Conclusions

A novel glass–mica composite seal was developed based on the previous concept of "infiltrated" mica seals for solid oxide fuel cells. A Ba–Al–Ca silicate sealing glass was mixed with Phlogopite mica flakes to form glass–mica composite seals with 10–50 vol.% glass. Short-term thermal cycling tests showed lower leak rates for higher glass contents. The 800 °C leak rates were ∼0.01 sccm cm^{-1} for composite seals with glass ≥30 vol.% when pressed at only 6 psi. The leak rates were about 4–5 times higher (∼0.04–0.05 sccm cm^{-1}) when the helium pressure was increased from 0.2 to 2 psi. Glass–mica composites with 10 and 20 vol.% of glass were also tested at low and high applied compressive stresses. It was found that the leak rate decreased with increasing compressive stress and with increasing glass content. Post mortem analyses were conducted on fracture surfaces. The fracture occurred mostly between mica flakes, but, the presence of fracture regions through the glass or at the glass/metal interface led to the observed increases in leak rate with increasing thermal cycles. The long-term OCV and thermal cycling test clearly demonstrated the desired sealing capability and the thermal cycle stability of the glass–mica composite seals.

Acknowledgements

The authors would like to thank S. Carlson for SEM sample preparation, and J. Coleman for SEM analysis. This paper was funded as part of the Solid-State Energy Conversion Alliance (SECA) Core Technology Program by the US Department of Energy's National Energy Technology Laboratory (NETL). Pacific Northwest National Laboratory is operated by Battelle Memorial Institute for the US Department of Energy under contract no. DE-AC06-76RLO 1830.

References

[1] S. Taniguchi, M. Kadowski, T. Yasuo, Y. Akiyama, Y. Miyake, K. Nishio, Improvement of thermal cycle characteristics of a planar-type solid oxide fuel cell by using ceramic fiber as sealing material, J. Power Sources 90 (2) (2000) 163–169.
[2] X. Qi, F.T. Akin, Y.S. Lin, Ceramic–glass composite high temperature seals for dense ionic-conducting ceramic membranes, J. Membr. Sci. 193 (1) (2001) 185–193.
[3] N. Lahl, D. Bahadur, K. Singh, L. Singheiser, K. Hilpert, Chemical interactions between aluminosilicate base sealants and the components on the anode side of solid oxide fuel cells, J. Electrochem. Soc. 149 (5) (2002) A607–A614.
[4] K. Ley, M. Krumpelt, J. Meiser, I. Bloom, Glass–ceramic sealants for solid oxide fuel cells. Part I. Physical properties, J. Mater. Res. 11 (6) (1996) 1489–1493.
[5] R. Zheng, S.R. Wang, H.W. Nie, T.-L. Wen, SiO_2–CaO–B_2O_3–Al_2O_3 ceramic glaze as sealant for planar ITSOFC, J. Power Sources 128 (2) (2004) 165–172.
[6] S.-B. Sohn, S.-Y. Choi, G.-H. Kim, H.-S. Song, G.-D. Kim, Stable sealing glass for planar solid oxide fuel cell, J. Non-Cryst. Solids 297 (1) (2002) 103–112.
[7] Y.-S. Chou, J.W. Stevenson, L.A. Chick, Ultra-low leak rate of hybrid compressive mica seals for solid oxide fuel cells, J. Power Sources 112 (1) (2002) 130–136.
[8] Y.-S. Chou, J.W. Stevenson, L.A. Chick, Novel compressive mica seals with metallic interlayers for solid oxide fuel cell applications, J. Am. Ceram. Soc. 86 (6) (2003) 1003–1007.
[9] S. Simner, J.W. Stevenson, Compressive mica seals for SOFC applications, J. Power Sources 102 (1–2) (2001) 310–316.
[10] Y.-S. Chou, J.W. Stevenson, Novel infiltrated Phlogopite mica compressive seals for solid oxide fuel cells, J. Power Sources 135 (1) (2004) 72–78.
[11] M. Bram, S. Peckers, P. Drinovac, J. Monch, R.W. Steinbrech, H.P. Buckkremer, D. Stover, Deformation behavior and leakage tests of alternate sealing materials for SOFC stacks, J. Power Sources 138 (1–2) (2004) 111–119.
[12] K.S. Weil, J.S. Hardy, J.Y. Kim, Use of a novel ceramic-to-metal braze for joining in high temperature electrochemical devices Joining of Advanced and Specialty Materials V, vol. 5, American Society of Metals, 2002, pp. 47–55.
[13] J. Duquette, A. Petric, Silver wire seal design for planar solid oxide fuel cell stack, J. Power Sources 137 (1) (2004) 71–75.
[14] W.B. Hanson, K.I. Ironside, J.A. Fernie, Active metal brazing of zirconia, Acta Meter. 48 (2000) 4673–4676.
[15] K.D. Meinhardt, L.R. Pederson, US Patent 6 430 966.
[16] W. Li, K. Hasinka, M. Seabaugh, S. Swartz, J. Lannutti, Curvature in solid oxide fuel cells, J. Power Sources 138 (1/2) (2004) 145–155.
[17] Y.-S. Chou, J.W. Stevenson, Thermal cycling and degradation mechanisms of compressive mica-based seals for solid oxide fuel cell applications, J. Power Sources 112 (1/2) (2002) 376–383.
[18] Y.-S. Chou, J.W. Stevenson, Long-term thermal cycling of Phlogopite mica-based compressive seals for solid oxide fuel cells, J. Power Sources 140 (2) (2005) 340–345.